A finite temperature theory of rotationally inelastic diffraction: H2, HD, and D2 on Cu(100)

Astrid J. Cruz and Bret Jackson

Citation: The Journal of Chemical Physics **91**, 4985 (1989); doi: 10.1063/1.456739
View online: http://dx.doi.org/10.1063/1.456739
View Table of Contents: http://scitation.aip.org/content/aip/journal/jcp/91/8?ver=pdfcov
Published by the AIP Publishing

A finite temperature theory of rotationally inelastic diffraction: H_2, HD, and D_2 on Cu(100)

Astrid J. Cruz and Bret Jackson
Department of Chemistry, University of Massachusetts, Amherst, Massachusetts 01003

(Received 9 May 1989; accepted 30 June 1989)

The rotationally inelastic diffraction probabilities for H_2, HD, and D_2 from Cu(100) were computed as a function of surface temperature. The surface is treated in a quantum mechanical fashion using a recently developed formalism. The center of mass molecular translational motion is treated semiclassically, using Gaussian wave packets (GWPs), and the rotations are described quantum mechanically. Strong attenuation of the phonon elastic diffraction peaks with temperature is observed. This Debye–Waller-like attenuation increases with increasing molecular mass and kinetic energy, and decreases as the peaks become more off-specular. The phonon summed rotation–diffraction probabilities show a moderate temperature dependence for the most part. The $0 \rightarrow 2$ rotational excitation of D_2 appears to be strongly phonon assisted above 300 K. At low temperatures our method reproduces the selection rules predicted by previous studies. As the temperature is increased these selection rules become less restrictive. The probability distribution for a scattering molecule exchanging an amount of energy ΔE with the surface was also computed. Rayleigh phonons were found to dominate the energy transfer, with bulk vibrations becoming more important for larger molecular masses, beam energies, and surface temperatures.

I. INTRODUCTION

A great deal of experimental effort has been focused on the interaction of H_2 and its isotopes with metal surfaces. In particular, several groups have examined such things as rotationally inelastic diffraction,[1–6] rotationally mediated selective adsorption,[6–9] and dissociative adsorption[10–12] on a number of metals. The scattering experiments are capable of providing detailed information on the final rotational state distribution,[1–6] as well as angular and time of flight data.[2,7,9,13] This in turn, can tell us a great deal about the molecule–surface interaction potential. In practice, one generally fits a model potential to the experimental findings, via some scattering theory. In order to get a proper fit to experiment, it is important that these scattering theories include the effects of finite surface temperature. That is, the scattering molecule must be able to exchange energy with the surface and bulk vibrations (phonons) of the solid. A recent study of the rotationally mediated selective adsorption of HD[14] on Cu included a weak (one phonon) coupling to these vibrations. However, there have been no quantum studies of the way in which temperature effects the rotationally inelastic diffraction of H_2. DePristo and co-workers[15] examined this system a few years ago, treating the molecular rotations quantum mechanically, and the translational motion classically. The vibrations of the surface were also treated classically, via the usual generalized Langevin techniques. However, this study ignored diffraction and did not examine the temperature dependence of the rotational transition probabilities in any detail. In addition, experiments have clearly shown that the primary mode of energy exchange for these light molecules is a very quantum mechanical single phonon event. Thus, it would be best to treat the lattice quantum mechanically.

In this work we present a detailed theoretical study of the rotationally inelastic diffraction of H_2, HD, and D_2 from Cu(100) as a function of surface temperature. The vibrations of the solid, and their coupling to the molecule are both treated in a fully quantum fashion, using a recently developed finite temperature formalism.[16] This formalism gives a good description of light molecule–surface energy transfer, and compared well with experimental studies of He and Ne scattering from Cu.[16,17] The molecular rotational motion is treated quantum mechanically, and the center of mass translation is treated semiclassically, via the use of the gaussian wave packets. This wave packet method has been shown to give good results for both rotation and diffraction probabilities for the scattering of H_2 from a corrugated surface[18] when compared with exact close coupled results.[19] The method should perform equally well or better for the heavier HD and D_2.

The rotation–diffraction peaks usually consist of a sharp phonon–elastic peak, with broad side bands due to phonon creation and absorption. Our approach provides us with a great deal of information about both the phonon elastic and inelastic states. Thus, we cannot only examine the temperature dependence of the central peak intensity, which is what is generally measured in experiments, but we can also compute the total probabilities for rotational excitation or diffraction. In this work we examine the intensity at each peak, its total (phonon elastic plus inelastic) probability, and the diffraction summed rotational probabilities. This allows us to distinguish between phonon assisted rotational excitation and Debye–Waller effects, which result from a thermal modulation of the beam coherence which gives rise to diffraction structure. We will also compute $P(\Delta E)$, the probability that a scattering molecule exchanges an amount of energy ΔE with the surface or bulk modes.

In Sec. II we briefly describe the model and its implementation. The results are presented and discussed in Sec. III, and we close with a brief summary in Sec. IV.

 0021-9606/89/204985-09$02.10

II. THEORY

A. The Hamiltonian

We begin by defining our total molecule plus solid Hamiltonian as

$$H = H_m^0 + H_b + V. \tag{1}$$

H_m^0 describes the molecule's translational and rotational degrees of freedom

$$H_m^0 = \frac{-\hbar^2}{2M}\nabla_R^2 + (2\mu r^2)^{-1}\mathscr{L}^2(\Theta,\phi), \tag{2}$$

where M and μ are the total and reduced mass of the molecule, respectively, $\vec{R}$ is the center of mass (COM) coordinate, and r is the bond length. $\mathscr{L}^2$ is the usual angular momentum operator, and Θ and ϕ are the polar and azimuthal orientation angles of the molecule. We have made the rigid rotor approximation, which is quite valid for the low translational energies of interest. The Hamiltonian for the bath (the phonons) is written in the usual fashion

$$H_b = \sum_q \hbar\omega_q \left[a_q^\dagger a_q + \tfrac{1}{2}\right], \tag{3}$$

where the operators $a_q^\dagger$ and a_q create and annihilate phonons of frequency ω_q and wave vector $\vec{q}$, respectively. The interaction between the diatomic and the atoms of the solid is taken to be

$$V = \sum_{i=1}^{2} D\, e^{-2\alpha[Z_i - Z_0 - W(\vec{R}_i,\{\vec{U}_s\})]} - V_{\rm att}(Z_i), \tag{4}$$

where $V_{\rm att} = 2De^{-\alpha(Z_i - Z_0)}$. The atoms of the diatomic are located at $\vec{r}_i$ $(i = 1,2)$, which consists of Z_i, the distance above the surface plane and $\vec{R}_i$, the position in the surface (X,Y) plane. The attractive part of V, $V_{\rm att}$, depends upon Z_i only. The instantaneous displacement of the surface atom at site s from its equilibrium position is given by $\vec{U}_s$. The corrugation function W describes how the turning point of an incoming molecule varies across the surface plane due to the corrugation and thermal fluctuations. At typical temperatures, it is reasonable to expand V in a Taylor series to first order in $\vec{U}_s$. The first term ($\vec{U}_s = 0$) is the molecule–static surface interaction

$$V_0 = \sum_{i=1}^{2} [f(\vec{r}_i) - V_{\rm att}(Z_i)], \tag{5}$$

where

$$f(\vec{r}_i) = De^{-2\alpha[Z_i - Z_0 - W(\vec{R}_i,0)]}. \tag{6}$$

The second term describes the molecule–bath (phonon) interaction:

$$V_{mb} = \sum_{i=1}^{2} 2\alpha f(\vec{r}_i) \sum_s \frac{dW}{d\vec{U}_s}\cdot\vec{U}_s. \tag{7}$$

The term $dW/d\vec{U}_s$ represents the variation of the turning point with respect to surface atom displacement. Bortolani *et al.*[20] have computed this term for He scattering from Cu(111), Au(111), and Ag(111), and found that effects due to displacements perpendicular to the surface were the most important, and of the form

$$\frac{dW(\vec{R}_i)}{dU_{sZ}} = A_Z \exp\left[\frac{-1}{2}Q_c^2|\vec{R}_i - \vec{R}_s|^2\right], \tag{8}$$

where $\vec{R}_s$ is the position vector of atom s in the surface plane. A_Z and Q_C are constants determined in their calculations. The perpendicular displacement is written in the usual way

$$U_{sZ} = N^{-1/2}\sum_q \left(\frac{\hbar}{2M_s\omega_q}\right)^{1/2} \exp(iQ\cdot R_s) \times e_z(q)(a_q + a_q^\dagger), \tag{9}$$

where M_s is the surface atom mass, Q is the X–Y component of the phonon wave vector $\vec{q}$, and $e_z(q)$ is the Z component of the phonon polarization vector. Substituting Eqs. (8) and (9) into Eq. (7) and performing the sum over s results in a gas–phonon interaction potential $V_{\rm mb}$ of the following form:[16,20–22]

$$V_{mb} = \frac{1}{\sqrt{N}}\sum_q S_q \Delta_Q(\vec{r}_1,\vec{r}_2)(a_q + a_q^\dagger), \tag{10}$$

where

$$\Delta_Q(\vec{r}_1,\vec{r}_2) = \sum_{i=1}^{2} f(\vec{r}_i)e^{iQ\cdot R_i} \tag{11}$$

and

$$S_q = 2\alpha\left(\frac{\hbar}{2M_s\omega_q}\right)^{1/2} A_Z e_Z(q)\left(\frac{2\pi}{AQ_c^2}\right)e^{-Q^2/2Q_c^2}, \tag{12}$$

where A is the area of the surface unit cell.

Our full Hamiltonian is now written

$$H = H_m + H_b + V_{\rm mb}, \tag{13}$$

where $H_m = H_m^0 + V_0$. In order to reproduce the corrugated Morse potential used in previous calculations,[18,19] we define $W(\vec{R}_i,0)$ for a (100) surface geometry in the following manner:

$$e^{2\alpha W(\vec{R}_i,0)} = 1 - \beta_i\left[\cos\frac{2\pi X_i}{c} + \cos\frac{2\pi y_i}{c}\right], \tag{14}$$

where $c = 2.55$ Å is the lattice spacing for Cu.

B. The wave function

We write the full gas–surface wave function as an expansion in all zero and one-phonon excitations, while maintaining a product state form:

$$|\Psi\rangle = |\Psi_m\rangle\left\{C_0(t) + \frac{1}{\sqrt{N}}\sum_q \left[C_{q+}(t)a_q^\dagger + C_{q-}(t)a_q\right]\right\} \times e^{-iE_l t/\hbar}|\{n_i\}\rangle, \tag{15}$$

where E_l is the lattice energy corresponding to the lattice state $|\{n_i\}\rangle$. The complex coefficients C_0, C_{q+}, and C_{q-} are related to the probability amplitudes for particles which scatter without exchanging energy with the surface, and those which excite or absorb phonons, respectively. This form for Ψ has been shown to give good results for light gas species, and is discussed in more detail elsewhere in the literature.[16]

The molecular wave function Ψ_m is described via a semiclassical technique[18,23–25] which has been successfully applied to the scattering of H_2 from a static surface.[18] The rotational motion is represented in a fully quantum fashion, via

an expansion in rotational eigenstates. The translational part of Ψ_m is written as a linear combination of Gaussian wave packets (GWP) $G_\alpha(\vec{R};t)$, where

$$G_\alpha(\hat{R};t) = \exp\{(i/\hbar)\{[\vec{R}-\hat{R}_\alpha(t)]\cdot\overleftrightarrow{A}(t)\cdot[\vec{R}-\vec{R}_\alpha(t)] + P_\alpha(t)\cdot[\vec{R}-\vec{R}_\alpha(t)]\}\}. \quad (16)$$

The time dependent parameters $\vec{R}_\alpha(t)$ and $\vec{P}_\alpha(t)$ are the average position and momentum of each packet, and $\overleftrightarrow{A}_\alpha(t)$ is related to the width. As in our earlier study[18] we write

$$\Psi_m(\vec{R},\Theta,\phi;t) = \sum_{\alpha=1}^{N} C_\alpha\, G_\alpha(\vec{R};t) \times \sum_{i=1}^{n} C_{\alpha i}(t)\, Y_i(\Theta,\phi) e^{-i\epsilon_i t/\hbar}, \quad (17)$$

where the index $i=(J,m_J)$ labels the spherical harmonic $Y_J^{m_J}(\Theta,\phi)$, and ϵ_i is the corresponding rotational energy $\epsilon_J = J(J+1)/2\mu r^2$. Initially, $(t=0)$, the N packets are arranged in a grid parallel to the surface, several angstroms above the metal, and covering a single surface unit cell. Heller has demonstrated[24] how by writing $C_\alpha = B\exp[(i/\hbar)\vec{P}_\alpha(0)\cdot\vec{R}_\alpha(0)]$, where B is a normalization constant, the sum of packets mimics a plane wave in X and Y. This gives our initial state the X–Y coherence necessary for diffraction. The above Ψ_m is a mean trajectory formulation in that each GWP is coupled to the full set of rotational states i. As each GWP evolves it drives the rotational state amplitudes $C_{\alpha i}(t)$. This method has been shown to work well for H_2, when compared with exact calculations.[18,19] The reader is referred to these earlier papers for more details.

C. Equations of motion

To obtain equations of motion for ψ_{ml} C_0, C_q^+, and C_q^- we introduce the full gas–surface wave function into the time dependent Schrödinger equation [using Eq. (13)] and project onto the states $\langle\{n_i\}|e^{iE_l t/\hbar}$, $\langle\{n_i\}|e^{iE_l t/\hbar}a_q$, and $\langle\{n_i\}|e^{iE_l t/\hbar}a_q^+$. Because we have chosen to include the extra coefficient $C_0(t)$, which is unneeded due to normalization of Ψ, we need an extra equation. We use

$$\frac{d}{dt}\langle\Psi_m|\Psi_m\rangle = 0. \quad (18)$$

In this way, both Ψ_m and the total wave function Ψ are normalized throughout the propagation. Thus, the phonon states also remain normalized at all times. That is

$$|C_0|^2 + \frac{1}{N}\sum_q [\,|C_{q+}|^2(n_q+1) + |C_{q-}|^2 n_q] = 1, \quad (19)$$

where $n_q = [\exp(\hbar\omega_q/kT)-1]^{-1}$, the thermal population of mode q at temperature T. The resulting equations of motion are

$$\dot{\Psi}_m = -\frac{i}{\hbar}H_m\Psi_m - \frac{i}{\hbar}\frac{1}{N}\sum_q [\Delta_Q - \langle\Psi_m|\Delta_Q|\Psi_m\rangle] \times\frac{1}{C_0}S_q[C_{q+}(n_q+1) + C_{q-}n_q], \quad (20)$$

$$\dot{C}_0(t) = -\frac{i}{\hbar}\frac{1}{N}\sum_q\langle\Psi_m|\Delta_Q|\Psi_m\rangle \times S_q[C_{q+}(n_q+1) + C_{q-}n_q], \quad (21)$$

$$\dot{C}_{q+}(t) = -i\omega_q C_{q+} - (i/\hbar)S_q C_0(t)\langle\Psi_m|\Delta_Q|\Psi_m\rangle, \quad (22)$$

$$\dot{C}_{q-}(t) = i\omega_q C_{q-} - (i/\hbar)S_q C_0(t)\langle\Psi_m|\Delta_Q|\Psi_m\rangle. \quad (23)$$

As in our previous study,[16] we simplify the above equations by replacing the Q in Δ_Q with an average value $\bar{Q}$;

$$\bar{Q}_\pm = \sum_q |C_{q\pm}(t)|^2 Q \sum_q |C_{q\pm}(t)|^2. \quad (24)$$

Thus, Δ_Q becomes $\bar{\Delta}$, and we only need to compute its average over Ψ_m once per integration step (along with Q_+ and Q_-). To obtain equations of motion for the time dependent parameters in Ψ_m, we rewrite H_m and $\bar{\Delta}$ in the COM coordinates, $\vec{R}$, Θ, and ϕ, insert Ψ_m [Eq. (17)] into Eq. (20), and operate from the left with

$$\int_0^{2\pi} d\phi \int_0^{\pi} d\Theta \sin\Theta\, Y_K^*(\Theta,\phi) e^{i\epsilon_K t/\hbar}.$$

This leads to

$$\sum_\alpha C_{\alpha k}(t)\left(\frac{\hbar^2}{2M}\nabla_R^2 + i\hbar\frac{\partial}{\partial t}\right)G_\alpha(\vec{R};t) + i\hbar\sum_\alpha G_\alpha(\vec{R};t)\dot{C}_{\alpha k}(t) = \sum_\alpha G_\alpha \sum_i C_{i\alpha}\, e^{-i(\epsilon_i-\epsilon_k)t/\hbar}V_{ki}(\vec{R}) + \sum_\alpha G_\alpha\sum_i C_{i\alpha}(t)\, e^{-i(\epsilon_i-\epsilon_k)t/\hbar} \times[\Delta_{ki}(\vec{R}) - \langle\Psi_m|\bar{\Delta}|\Psi_m\rangle] \times\frac{1}{C_0}\frac{1}{N}\sum_q S_q[C_{q+}(n_{q+}+1) + C_{q-}n_q], \quad (25)$$

where

$$V_{ki}(\vec{R}) = \int_0^{2\pi}\int_0^{\pi} d\phi\, d\Theta \sin\Theta\, Y_k^* V_0(R,\Theta,\phi) Y_i$$

and

$$\Delta_{ki}(\vec{R}) = \int_0^{2\pi}\int_0^{\pi} d\phi\, d\Theta \sin\Theta\, Y_k^*\bar{\Delta}(R,\Theta,\phi) Y_i.$$

To solve the above equation, we again use the method proposed by Heller,[23,24] which expands V_{Ki} and Δ_{Ki} to second order in a Taylor series with respect to $(\vec{R}-\vec{R}_\alpha)$, for each packet. By equating equal powers of $(\vec{R}-\vec{R}_\alpha)$, one finds that the GWPs decouple and obey the following equations of motion:

$$\dot{\overleftrightarrow{A}}_\alpha = \left(\frac{-2}{M}\right)\overleftrightarrow{A}_\alpha(t)\cdot\overleftrightarrow{A}_\alpha(t) - \frac{1}{2}\sum_k\sum_i C_{\alpha k}^* C_{\alpha i}\, e^{-i(\epsilon_i-\epsilon_k)t/\hbar}\frac{\partial^2\overleftrightarrow{V}_{ki}(R_\alpha)}{\partial R_\alpha \partial R'_\alpha} - \frac{1}{2}\sum_k\sum_i C_{\alpha k}^* C_{\alpha i}\, e^{-i(\epsilon_i-\epsilon_k)t/\hbar}\frac{\partial^2\overleftrightarrow{\Delta}_{ki}(R_\alpha)}{\partial R_\alpha\partial R'_\alpha}\frac{1}{C_0}\frac{1}{N}\sum_q S_q[C_{q+}(n_q+1) + C_{q-}n_q], \quad (26)$$

$$\dot{\vec{R}}_\alpha(t) = \vec{P}_\alpha(t)/M, \tag{27}$$

$$\dot{\vec{P}}_\alpha(t) = -\sum_i \sum_k C^*_{\alpha k}\, C_{\alpha i}\, e^{-i(\epsilon_i-\epsilon_k)t/\hbar} \frac{\partial \vec{V}_{Ki}(R_\alpha)}{\partial R_\alpha} - \sum_i \sum_k C^*_{\alpha k} C_{\alpha i}\, e^{-i(\epsilon_i-\epsilon_k)t/\hbar} \frac{\partial \vec{\Delta}_{ki}(R_\alpha)}{\partial R_\alpha} \frac{1}{C_0} \frac{1}{N} \sum_q S_q \left[C_{q+}\,(n_q+1) + C_q n_q \right], \tag{28}$$

$$i\hbar \dot{C}_{\alpha K} = \left[\frac{1}{2M} \vec{P}_\alpha \cdot \vec{P}_\alpha - \vec{P}_\alpha \cdot \dot{\vec{R}}_\alpha - \frac{i\hbar}{M} \mathrm{Tr}\, \overleftrightarrow{A} \right] C_{\alpha K} + \sum_i C_{\alpha i}\, e^{-i(\epsilon_i-\epsilon_k)t/\hbar} V_{Ki}(R_\alpha) + \sum_i C_{\alpha i}\, e^{-i(\epsilon_i-\epsilon_k)t/\hbar} \Delta_{Ki}(R_\alpha) \frac{1}{C_0} \frac{1}{N} \sum_q S_q \left[C_{q+}\,(n_{q+}+1) + C_{q-}\, n_q \right] - \langle \Psi_m | \bar{\Delta} | \Psi_m \rangle \frac{C_{\alpha K}}{C_0} \frac{1}{N} \sum_q S_q \left[C_{q+}\,(n_q+1) + C_{q-}\, n_q \right]. \tag{29}$$

Both V_0 and $\bar{\Delta}$ are easily factored into products of $\vec{R}$-dependent terms and Θ-, ϕ-dependent terms. Thus, all of the necessary spherical harmonic matrix elements can be computed numerically prior to the running of the GWP trajectories. All of the V_{Ki} and Δ_{Ki} derivatives are easily computed analytically, as is the $\vec{R}$-dependent part of $\langle \Psi_m | \bar{\Delta} | \Psi_m \rangle$. Thus, there are no numerical integrations required to evolve the system, and computer requirements are minimal.

Note that the GWP equations of motion reduce to those of Jackson and Metiu[18] in the static surface limit ($\bar{\Delta} = 0$). Thus, the inclusion of V_{mb} gives rise to extra temperature dependent terms in $\overleftrightarrow{A}$, $\dot{\vec{P}}$, and $\dot{C}_{\alpha i}$ due entirely to the molecule–phonon interaction. Initially ($t = 0$), the molecule is far above the surface and the amplitudes for phonon excitation and absorption are zero; that is, $C_{q+}(0) = C_{q-}(0) = 0$, and $C_0 = 1$. The molecule is in the $J = m_J = 0$ rotational state and the $C_{\alpha i}$'s corresponding to all other states are zero. As the GWPs are evolved (simultaneously) towards the surface, both the excited state rotational amplitudes $C_{\alpha i}$ and the phonon amplitudes $C_{q\pm}$ become nonzero. This in turn "activates" the phonon terms in the equations of motion, modifying the gas–surface potential and causing the GWPs to speed up or slow down as necessary, to conserve total energy. The phonon amplitudes and the GWPs are evolved simultaneously and self consistently, until the packets have emerged from the interaction region. Our choice for the initial value of the A matrix is the same as in our earlier paper.[18]

In this study we consider both bulk and surface (Rayleigh) phonons. That is, we make the replacement

$$\frac{1}{N}\sum_q \rightarrow \frac{1}{N_b}\sum_K + \frac{1}{N_r}\sum_\lambda,$$

where K denotes the wave vector of the N_b bulk modes and λ labels the N_r Rayleigh modes. This replacement results in a separate set of C_+ and C_- amplitudes for each type of mode. The dispersion relations and polarization vectors for Rayleigh and bulk modes are the same as used previously.[16,26] For the Rayleigh modes, we used 110 values for Q, and for the bulk modes we used 70 values for Q and 70 values for q_z, the z component of $\vec{q}$.

D. Final state examination

As discussed in detail in the static surface study,[18] we compute $P_{nm}^{Jm_J}$ the probability of scattering into the final rotational state (J,m_J) and diffraction state (n,m), from the S-matrix in the usual fashion. That is, $P_{nm}^{Jm_J} = |S_{nm}^{Jm_J}|^2$, where $S_{nm}^{Jm_J}$ is the projection of our final Ψ_m onto $e^{iK_{nmJ}\cdot R} Y_J^{m_J}$, where the final wave vector K_{nmJ} is determined from the initial beam momentum, the reciprocal lattice vectors, and the energies ϵ_i via conservation of energy. The zero-phonon component of this state (which is what one generally measures) is given by

$$I_{nm}^{Jm_J} = P_{nm}^{Jm_J} |C_0|^2. \tag{30}$$

Note that both $P_{nm}^{Jm_J}$ and C_0 are temperature dependent. The term $|C_0|^2$ is primarily responsible for the Debye–Waller thermal attenuation of the observed diffraction peaks. The probability of scattering into the (J,m_J,n,m) state and exciting a phonon of wave vector $\vec{q}$ is given by

$$P_{nm}^{Jm_J} \frac{1}{N} |C_{q+}|^2 (n_q+1). \tag{31}$$

Thus, the probability that a molecule excites a phonon of frequency ω_q and loses an amount of energy $|\Delta E| = \hbar\omega_q$, is

$$P(\Delta E = -\hbar\omega_q) = \frac{1}{N} |C_{q+}(t)|^2 (n_q+1) \tag{32}$$

with a similar expression for the absorption of phonons.

III. RESULTS AND DISCUSSION

In this section we present results for the scattering of H_2, D_2 and HD from a Cu(100) surface. The rotationally inelastic diffraction probabilities and the energy transfer probabilities were computed for an incident beam energy of 50 meV, a normal angle of incidence and several surface temperatures between 10 and 450 K. Nordlander, Holmberg and Harris[27] have computed the H_2–surface interaction potential for a variety of noble metals, including Cu(110). We thus choose our parameters by fitting our potential to their results, taking $\alpha = 1.0$ Å^{-1}, $D = 24$ meV, and $Z_0 = 2.5$ Å. The maximum phonon frequency for the bulk modes is 240 cm^{-1}. For the Rayleigh phonons we use the available data for Cu(111)[26] as an approximation for the (100) face, choosing

$\omega_{max} = 113\ cm^{-1}$. Once again we use the values $A_Z = 0.6$ and $Q_C = .72\ Å^{-1}$ as computed by Bortolani and coworkers.[20] In order to compare with some earlier calculations which used a purely repulsive potential,[18,19] we set $V_{att} = 0$ for the calculations presented here. The corrugation parameter β was 0.1.

In Fig. 1 we plot the phonon-elastic peak heights $I_{nm}^{Jm_J}$ vs temperature. The attenuation of I_{00}^{00} with temperature is slightly faster than exponential, as is seen experimentally for H_2 and other light molecule–metal systems.[5,7,9(b),17] By varying our potential parameters, one could probably fit these results to experiment, although we make no effort to do so here. The specular peak height (I_{00}^{00}) for H_2 was computed for two initial beam energies, and it is clear that thermal attenuation (phonon inelasticity) increases with beam energy, as expected. By comparing I_{00}^{00} for H_2, HD, and D_2, it is also clear that this decay rate increases with molecular mass. Off-specular diffraction peaks and rotationally inelastic peaks behave in a similar fashion, and a few examples are shown in Fig. 1. All of this behavior is consistent with the usual Debye–Waller-type models.[28]

Note that by 300 K, much of the final scattered state is phonon inelastic. Note also that the ratio of any two peak heights is not a constant with temperature. Thus, if we want to fit a potential to experimental results, we must take temperature into consideration.

In order to simplify our results we present the final state probabilities $P_{nm}^{Jm_J}$ for H_2, HD, and D_2 in Tables I–III, respectively. $P_{nm}^{Jm_J}$ is proportional to the total rotation–diffractin peak area summed over all final phonon states, and does not include the strong Debye–Waller thermal attenuation. To further simplify our discussion we list the diffraction summed probabilities P^{Jm_J}, where

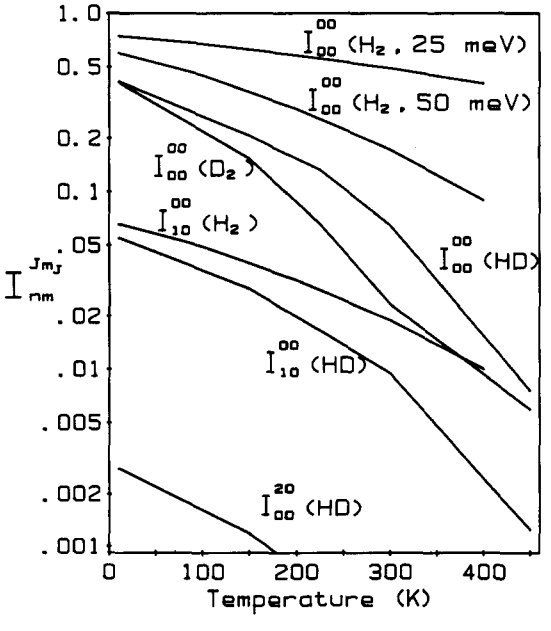

FIG. 1. Elastic peak heights $I_{nm}^{Jm_J}$ vs temperature for H_2, HD, and D_2 scattered from Cu(100) at normal incidence. The beam energy is 50 meV unless otherwise noted.

TABLE I. Transitions probabilities $P_{nm}^{Jm_J}$ for H_2 scattered from Cu(100). $\beta = 0.1$, $E_i = 50$ meV, at different surface temperatures.

		$\|J,m_J\rangle$			
(n,m)	T(K)	$\|0,0\rangle$	$\|2,0\rangle$	$\|2,1\rangle$	$\|2,2\rangle$
(0,0)	10	0.667	0.535(−4)	0.561(−13)	0.279(−16)
	100	0.668	0.494(−4)	0.255(−12)	0.166(−15)
	300	0.665	0.404(−4)	0.298(−11)	0.963(−15)
	400	0.657	0.364(−4)	0.758(−11)	0.168(−14)
(1,0)	10	0.737(−1)			
	100	0.732(−1)	...	...	...
	300	0.729(−1)			
	400	0.736(−1)			
(1,1)	10	0.328(−2)			
	100	0.342(−2)	...	...	...
	300	0.402(−2)			
	400	0.451(−2)			
(0,2)	10	0.594(−2)			
	100	0.600(−2)	...	...	...
	300	0.647(−2)			
	400	0.714(−2)			

$$P^{Jm_J} = \sum_n \sum_m P_{nm}^{Jm_J},$$

in Tables IV–VI for H_2, HD, and D_2, respectively.

For H_2, off-specular scattering is not energetically allowed for $\Delta J = 2$. It is interesting to note the influence of thermal fluctuations on selection rules which arise from lattice symmetry. Proctor, Kouri, and Gerber[29] have shown that for square lattices, the $\Delta m_J = \pm 1 \pm 2$ transitions are not allowed for the specular peak ($n = 0, m = 0$.) At 10 K, all of our probabilities are on the order of 10^{-11} or less for these transitions, in agreement with their results. As temperature is raised, however, these probabilities increase rapidly. At higher temperatures, the vibrational amplitudes of the surface atoms increase, giving rise to a larger asymmetries in the instantaneous surface geometry, and easing the selection rules. For the heavier D_2, the molecule–phonon coupling is the largest, and the largest increase in P_{00}^{21} and P_{00}^{22} is seen.

For H_2, the variation of $P_{nm}^{Jm_J}$ with temperature is small. This is expected, since H_2 has a low mass and the molecule–phonon coupling is weak. The probability for rotational excitation is small because the energy required (45 meV) is large, and only slightly less than the beam energy. This energy is also much larger than the phonon energies, and they play a minor role in rotational excitation. Note that the (1,1) and (0,2) probabilities increase with temperature, (1,0) is fairly constant, and P_{00}^{00} decreases. Thus, I_{00}^{00} decays more rapidly with temperature than I_{10}^{00}, which is faster than I_{11}^{00} and I_{02}^{00}. This is also consistent with Debye–Waller arguments[28] which suggest that the thermal attenuation increases with $|\Delta k_Z|^2$, where Δk_Z is the change in the Z-com-

TABLE II. Same as Table I, except for HD/Cu(100).

		$\|Jm_J\rangle$					
(n,m)	T(K)	$\|0,0\rangle$	$\|1,0\rangle$	$\|1,1\rangle$	$\|2,0\rangle$	$\|2,1\rangle$	$\|2,2\rangle$
(0,0)	10	0.477	0.163	0.451(−10)	0.321(−2)	0.149(−10)	0.184(−14)
	150	0.473	0.158	0.787(−9)	0.272(−2)	0.223(−9)	0.417(−13)
	300	0.462	0.153	0.324(−8)	0.228(−2)	0.948(−9)	0.178(−12)
	450	0.422	0.153	0.517(−8)	0.227(−2)	0.289(−8)	0.983(−12)
(1,0)	10	0.634(−1)	0.141(−1)	0.926(−4)	0.572(−4)	0.466(−5)	0.202(−5)
	150	0.652(−1)	0.143(−1)	0.829(−4)	0.539(−4)	0.337(−5)	0.166(−5)
	300	0.674(−1)	0.152(−1)	0.730(−4)	0.578(−4)	0.237(−5)	0.137(−5)
	450	0.692(−1)	0.181(−1)	0.644(−4)	0.825(−4)	0.192(−5)	0.120(−5)
(1,1)	10	0.626(−2)	0.998(−3)	0.122(−4)	0.171(−5)	0.743(−7)	0.697(−8)
	150	0.663(−2)	0.101(−2)	0.117(−4)	0.117(−5)	0.669(−7)	0.453(−8)
	300	0.734(−2)	0.114(−2)	0.116(−4)	0.102(−5)	0.708(−7)	0.295(−8)
	450	0.852(−2)	0.154(−2)	0.126(−4)	0.150(−5)	0.937(−7)	0.215(−8)

TABLE III. Same as Table I, except for D_2/Cu(100).

		$\|J,m_J\rangle$			
(n,m)	T(K)	$\|0,0\rangle$	$\|2,0\rangle$	$\|2,1\rangle$	$\|2,2\rangle$
(0,0)	10	0.488	0.347(−2)	0.117(−11)	0.222(−13)
	150	0.478	0.362(−2)	0.250(−10)	0.586(−12)
	300	0.455	0.444(−2)	0.350(−9)	0.394(−11)
	450	0.748	0.677(−1)	0.307(−6)	0.176(−9)
(1,0)	10	0.102	0.375(−3)	0.786(−5)	0.198(−4)
	150	0.103	0.401(−3)	0.798(−5)	0.215(−4)
	300	0.104	0.528(−3)	0.954(−5)	0.293(−4)
	450	0.201(−1)	0.497(−2)	0.163(−3)	0.192(−3)
(1,1)	10	0.158(−1)	0.266(−4)	0.138(−5)	0.204(−7)
	150	0.169(−1)	0.312(−4)	0.144(−5)	0.204(−7)
	300	0.188(−1)	0.467(−4)	0.183(−5)	0.232(−7)
	450	0.337(−2)	0.485(−3)	0.157(−4)	0.707(−7)
(2,0)	10	0.685(−2)	0.137(−4)	0.322(−6)	0.101(−5)
	150	0.713(−2)	0.131(−4)	0.306(−6)	0.111(−5)
	300	0.857(−2)	0.187(−4)	0.385(−6)	0.179(−5)
	450	0.538(−2)	0.673(−3)	0.141(−4)	0.265(−4)

TABLE IV. Diffraction summed rotational transitions probabilities for H_2/Cu (100); $E_i = 50$ meV, $\beta = 0.1$, at several surface temperatures.

	Surface temperature (K)			
$\|J,m_J\rangle$	10K	100K	300K	400K
$\|0,0\rangle$	0.9999	0.9999	0.9999	0.9999
$\|2,0\rangle$	0.535(−4)	0.494(−4)	0.404(−4)	0.364(−4)
$\|2,1\rangle$	0.561(−13)	0.255(−12)	0.298(−11)	0.758(−11)
$\|2,2\rangle$	0.279(−16)	0.166(−15)	0.963(−15)	0.168(−14)

TABLE V. Same as Table IV, except for HD/Cu (100).

	Surface temperature (K)			
$\|J,m_J\rangle$	10K	150K	300K	450K
$\|0,0\rangle$	0.770	0.776	0.778	0.762
$\|1,0\rangle$	0.225	0.221	0.219	0.235
$\|1,1\rangle$	0.443(−3)	0.399(−3)	0.357(−3)	0.328(−3)
$\|2,0\rangle$	0.344(−2)	0.293(−2)	0.250(−2)	0.259(−2)
$\|2,1\rangle$	0.190(−4)	0.139(−4)	0.100(−4)	0.834(−5)
$\|2,2\rangle$	0.810(−5)	0.668(−5)	0.556(−5)	0.494(−5)

ponent of the wave vector of the scattering particle. The slight decrease of P_{00}^{20} with temperature probably results from a small thermal renormalization of V_0.

For HD, the gas-phonon coupling is a little larger, and the results are a bit more complicated, but not greatly different than for H_2. As for H_2, the probability shifts away from the specular peak at higher temperatures, and $I_{nm}^{Jm_J}$ decays less rapidly as the peaks become more off-specular. For the specular manifold, the $J=0\rightarrow1$ and $J=0\rightarrow2$ transitions decay slightly with temperature, except for the "forbidden" $\Delta m_J=\pm1,\ \pm2$ transitions. For the $(\pm1,0)$ and $(0,\pm1)$ peaks, the $J=0\rightarrow1$ and $0\rightarrow2$ transition probabilities increase by 28% and 44% ($\Delta m=0$) as T is raised from 10 to 450 K. For the $(\pm1,\pm1)$ peaks, $J=0\rightarrow1$ increases by 54% in this range, while other ΔJ changes are small.

A clearer picture of the rotational behavior is given in Table V. The total $J=0$ population actually rises with T and then drops. The $J=1$, $m_J=0$ state population drops slightly and then rises, at the expense of the much weaker $J=0\rightarrow2$ transition. The $\Delta m_J\neq0$ transition probabilities all decrease with T (again, except for the forbidden transitions), perhaps due to a thermal averaging or smoothing of the surface corrugation.

For D_2, the coupling to the phonons is even larger, and the energy of the $J=0\rightarrow2$ excitation is only 22 meV, which is less than half the beam energy, and between the surface and bulk phonon Debye frequencies. We thus see a very strong increase in the $J=0\rightarrow2$ transition for $kT>22$ meV ($T>260$ K), due to phonon assisted rotational excitation. This is true for all diffraction states, and appears to be independent of Δm_J, except for the "not allowed" (0, 0) peaks. Oddly enough, even though the $J=0$ probability decreases with T (as expected), P_{00}^{00} increases at high temperatures. That is, within the $J=0$ manifold, scattering slowly shifts

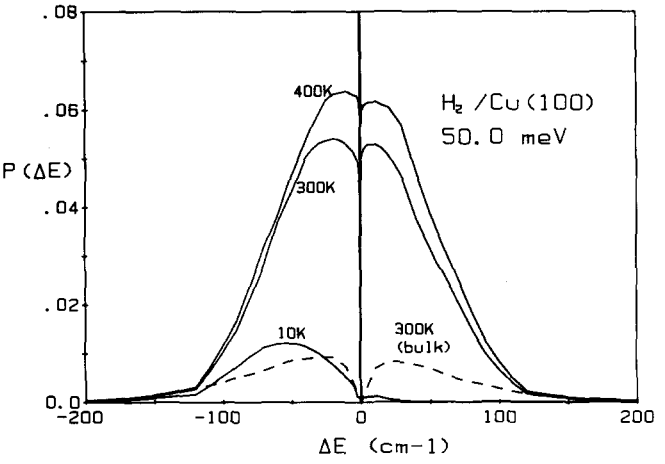

FIG. 2. Probability distribution for exchanging an amount of energy ΔE with the metal, for a 50 meV beam of H_2 scattered at normal incidence from Cu(100), at the temperatures indicated. The dotted line corresponds to the bulk phonon contribution at 300 K.

towards the off-specular as T increases (as for H_2 and HD), until about 300 K, when the situation is strongly reversed.

In Figs. 2–4, we plot $P(\Delta E)$, the probability that a scattering molecule exchanges an amount of energy ΔE with the phonons, for H_2, HD, and D_2, respectively. The results are for a beam energy of 50 meV, normal incidence, and the three surface temperatures indicated. Note that at 10 K most of the scattering is phonon elastic, with a small sideband due to phonon excitation (energy loss). This sideband is larger for heavier gas species. It is the sharp central peak that is usually measured. For H_2, the elastic intensity drops from 94.4% at 10 K to 36.7% at 400 K. For HD and D_2, the elastic probability is 13.3% and 8.9%, respectively, at 450 K. Thus, most of the scattering is phonon inelastic at higher temperatures. As temperature increases, a sideband due to energy gain (phonon absorption) appears and grows. By room temperature, energy loss and gain features are similar. As seen in earlier studies of He and Ne, phonon inelasticity increases with T, molecular mass, and beam energy.[16,21(b),22]

The dotted lines in Figs. 2–4 corresponds to the inelastic component arising from an interaction with the bulk vibrations. The remainder is due to the surface Rayleigh modes, which clearly dominate the energy transfer due to their large amplitude at the surface. Note that all energy transfer for $|\Delta E|>113\ \text{cm}^{-1}$ is due to the bulk modes. The bulk modes become more important for larger molecular energies and masses, and higher surface temperatures.[16,21(b),22]

TABLE VI. Same as Table IV, except for D_2/Cu (100).

	Surface temperature (K)			
$\|J,m_J\rangle$	10K	150K	300K	450K
$\|0,0\rangle$	0.995	0.994	0.993	0.904
$\|2,0\rangle$	0.513(−2)	0.540(−2)	0.684(−2)	0.931(−1)
$\|2,1\rangle$	0.384(−4)	0.390(−4)	0.473(−4)	0.752(−3)
$\|2,2\rangle$	0.836(−4)	0.910(−4)	0.125(−3)	0.870(−3)

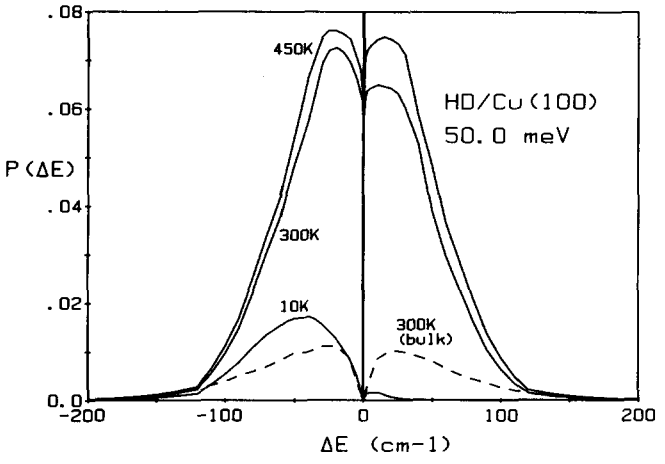

FIG. 3. Same as Fig. 2, except for HD.

IV. SUMMARY

In conclusion, we have developed a method for looking at the rotationally inelastic diffraction of diatomics from finite temperature surfaces. Each calculation requires only a few hours of CPU time on a Celerity 1260 D minicomputer. The semiclassical formalism used to treat the molecular degrees of freedom has been shown to work well for H_2 scattered from a static lattice. Similarly, the methodology for introducing finite temperature has been shown to give good results for light gas species.

At very low temperatures, our methods reproduced the selection rules ($\Delta m_J \neq \pm 1, \pm 2$) predicted by Proctor, Kouri, and Gerber[29] for homonuclear diatomics on square lattices. We also saw that these rules are obeyed for HD. As the temperature is raised, these selection rules become somewhat less restrictive, particularly for the heavier D_2, which couples more strongly to the phonons.

The addition of temperature introduces several effects. The first is a strong Debye–Waller-like attenuation of all phonon-elastic peaks with temperature. This attenuation rate decreases as the peaks become more off-specular (smaller $|\Delta k_Z|$). The attenuation increases with increasing molecular mass and kinetic energy. A thermal renormalization of the molecule–surface potential also occurs, which leads to small shifts in the various rotation–diffraction state probabilities with temperature. For H_2 and HD at low or moderate beam energies, these are the primary effects. For D_2, the coupling to the phonons is larger and the energy of the $\Delta J = 2$ transition is comparable to the phonon Debye frequencies. Thus, for $T > 300$ K or so, we see strong evidence of phonon assisted rotational excitation. This effect dominates the scattering behavior at room temperature and above.

This theory can be modified to include the gas–surface attraction, V_{att}, or more complex potentials in general. It is hoped that it can be used, in combination with experimental scattering results, to extract more realistic molecule–surface interaction potentials. Ways of replacing the semiclassical treatment of the molecule with a more exact time dependent method, such as the close coupled wave packet approach of Kouri and co-workers,[30] are being examined.

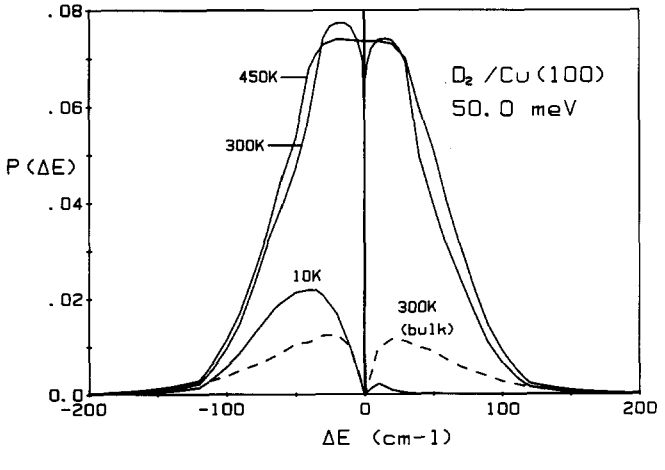

FIG. 4. Same as Fig. 2, except for D_2.

ACKNOWLEDGMENTS

This work was supported in part by the Division of Chemical Sciences, Office of Basic Energy Sciences, Office of Energy Research, U.S. Department of Energy, under Grant No. DE-FG02-87ER13744.

[1] E. E. Marinero, C. T. Rettener, and R. N. Zare, Phys. Rev. Lett. **48**, 1323 (1982); E. E. Marinero, R. Vasudev, and R. N. Zare, J. Chem. Phys. **78**, 692 (1983); S. L. Anderson, G. D. Kubiak, and R. N. Zare, Chem. Phys. Lett. **105**, 22 (1984); G. O. Sitz, A. C. Kummel, and R. N. Zare, J. Chem. Phys. **87**, 3247 (1987).
[2] G. Brusdeylins and J. P. Toennies, Surf. Sci. **126**, 647 (1983); W. Allison and B. Feuerbacher, Phys. Rev. Lett. **45**, 2040 (1980).
[3] G. Brusdeylins, G. Drolshagen, A. Kaufhold, J. Skofronick, and J. P. Toennies, Surf. Sci. **189/190**, 972 (1987); R. Horne and L. J. F. Hermans, Phys. Rev. Lett. **60**, 2777 (1988).
[4] G. Boato, P. Cantini, and L. Mattera, J. Chem. Phys. **65**, 544 (1976).
[5] J. P. Cowin, C. F. Yu, S. J. Sibener, and L. Wharton, J. Chem. Phys. **79**, 3537 (1983).
[6] C. F. Yu, C. S. Hogg, J. P. Cowin, K. B. Whaley, J. C. Light, and S. J. Sibener, Isr. J. Chem. **22**, 305 (1982).
[7] U. Harten, J. P. Toennies, and Ch. Woll, J. Chem. Phys. **85**, 2249 (1986).
[8] S. Anderson, L. Wilzen, and J. Harris, Phys. Rev. Lett. **55**, 2591 (1985); **57**, 1603 (1986).
[9] (a) C. F. Yu, K. B. Whaley, C. S. Hogg, and S. J. Sibener, Phys. Rev. Lett. **51**, 2210 (1983); J. P. Cowin, C. F. Yu, S. J. Sibener, and J. E. Hurst, J. Chem. Phys. **75**, 1033 (1981); (b) C. F. Yu, K. B. Whaley, C. S. Hogg, and S. J. Sibener, *ibid* **83**, 4217 (1985).
[10] A. V. Hamza and R. J. Madix, J. Phys. Chem. **89**, 5381 (1985); D. O. Hayward and A. O. Taylor, Chem. Phys. Lett. **124**, 264 (1986).
[11] H. J. Robota, W. Vielhaber, M. C. Lin, J. Senger, and G. Ertl, Surf. Sci. **155**, 101 (1985).
[12] H. P. Steinrück, M. Luger, A. Winkler, and K. D. Rendulic, Phys. Rev. B **32**, 5032 (1985); H. D. Steinrück, K. D. Rendulic, and A. Winkler, Surf. Sci. **154**, 99 (1985); H. Karner, M. Luger, H. P. Steinrück, A. Winkler, and K. D. Rendulic *ibid.* **163**, L641 (1985).
[13] J. P. Toennies, Annu. Rev. Phys. Chem. **27**, 225 (1976).
[14] M. D. Stiles and J. W. Wilkins, Phys. Rev. Lett. **54**, 595 (1985); M. D. Stiles, J. W. Wilkins, and M. Persson, Phys. Rev. B **34**, 4490 (1986).
[15] A. E. DePristo, Surf. Sci. **137**, 130 (1984).
[16] B. Jackson, J. Chem. Phys. **89**, 2473 (1988).
[17] J. Lapujoulade, Y. Lejay, and G. Armand, Surf. Sci. **95**, 107 (1980).
[18] B. Jackson and H. Metui, J. Chem. Phys. **84**, 3535 (1986).
[19] J. V. Lill and D. J. Kouri, Chem. Phys. Lett. **112**, 249 (1984).
[20] V. Bortolani, A. Franchini, N. Garciá, F. Nizzoli, and G. Santoro, Phys. Rev. B **28**, 7358 (1983).

[21](a) V. Bortolani, A. Franchini, F. Nizzoli, G. Santoro, G. Benedek, and V. Celli, Surf. Sci. **128**, 249 (1983); V. Celli, G. Benedek, U. Harten, J. P. Toennies, R. B. Doak, and V. Bortolani, *ibid.* **143**, L376 (1984); (b) B. Jackson, J. Chem. Phys **90**, 140 (1989).
[22]B. Jackson, J. Chem. Phys. **88**, 1383 (1988).
[23]E. J. Heller, J. Chem. Phys. **62** 1544 (1975); **65**, 4979(1976); K. C. Kulander and E. J. Heller, *ibid.* **69**, 2439 (1978); E. J. Heller, *ibid.* **68**, 2066, 3891 (1978).
[24]G. Drolshagen and E. Heller, J. Chem. Phys. **79**, 2072 (1983); Surf. Sci. **139**, 260 (1984).
[25]B. Jackson and H. Metui, J. Chem. Phys. **85**, 4129 (1986); **83**, 1952 (1985).
[26]D. Eichenauer, U. Harten, J. P. Toennies, and V. Celli, J. Chem. Phys. **86**, 3693 (1987); J. P. Toennies, in *Dynamics of Gas Surface Interaction*, edited by G. Benedek and U. Valbusa (Springer, New York, 1982).
[27]P. Nordlander, C. Holmberg, and J. Harris, Surf. Sci. **152/153**, 702 (1985).
[28]W. H. Weinberg, J. Chem. Phys. **57**, 5463 (1972); J. Phys. C **5**, 2098 (1972); J. L. Beeby, *ibid.* **5**, 3438 (1972); G. Comsa, *ibid.* **6**, 2648 (1973); A. C. Levi and H. Suhl, Surf. Sci. **88**, 221 (1979).
[29]T. R. Proctor, D. J. Kouri, and R. B. Gerber, J. Chem. Phys. **80**, 3845 (1984).
[30]R. C. Mowrey and D. J. Kouri, Chem. Phys. Lett. **119**, 285 (1985); J. Chem. Phys. **84**, 6466 (1986); R. C. Mowrey, H. F. Bowen, and D. J. Kouri, J. Chem. Phys. **86**, 2441 (1987).